



Therapeutic efficacy of rifaximin loaded tamarind gum polysaccharide nanoparticles in TNBS induced IBD model Wistar rats

Maria John Newton Amaldoss^{*1-3}, Imtiyaz Ahmed Najar^{*3}, Jatinder Kumar⁴, Archana Sharma³

¹Australian Centre for Nanomedicine, University of New South Wales, Sydney, NSW 2052, Australia

²Lowy Cancer Research Centre, Prince of Wales Clinical School, University of New South Wales, Sydney, NSW 2052, Australia

³Swift School of Pharmacy Rajpura, Punjab, India

⁴Rayat Bahra University, Hoshiarpur, Punjab, India

ABSTRACT

Background: Rifaximin is a non-systemic antibiotic used in the treatment of inflammatory bowel disease (IBD). Antibiotics are demonstrating a significant role in the treatment of IBD by altering the dysbiotic colonic microbiota and decreases the immunogenic and inflammatory response in the patient population. Mucoadhesive colon targeted nanoparticles provide the site-specific delivery and extended stay in the colon. Since the bacteria occupy the lumen, spread over the surface of epithelial cells, and adhere to the mucosa, delivering the rifaximin as a nanoparticles with the mucoadhesive polymer enhances the therapeutic efficacy in IBD. The objective was to fabricate and characterize the rifaximin loaded tamarind gum nanoparticles and study the therapeutic efficacy in the TNBS-induced IBD model rats

Materials and methods: The experimentation includes fabrication and characterization of drug excipient compatibility by FTIR. The fabricated nanoparticles were characterized for the hydrodynamic size and zeta potential by photon correlation spectroscopy and also analyzed by TEM. Selected best formulation was subjected to the therapeutic efficacy study in TNBS-induced IBD rats, and the macroscopic, microscopic and biochemical parameters were reported.

Results: The study demonstrated that the formulation TGN1 is best formulation in terms of nanoparticle characterization and hydrodynamic size which showed the hydrodynamic size of 171.4 nm and the zeta potential of -26.44 mV and other parameters such as TEM and drug release studies were also reported.

Conclusions: The therapeutic efficacy study revealed that TGN1 is efficiently reduced the IBD inflammatory conditions as compared to the TNBS control group and reference drug mesalamine group.

Key words: IBD; rifaximin; nanoparticles; tamarind gum

Rep Pract Oncol Radiother 2021;26(5):712-729

Introduction

Inflammatory bowel disease (IBD) is an auto-immune disorder characterized by inflammatory conditions associated with mucosal ulceration,

oedema and haemorrhage of the gastrointestinal tract (GIT) [1-3]. The prime objective of the IBD therapy is remission and maintenance of remission; however, an effective treatment is still challenging [4]. Although the standard treatment methods are

Address for correspondence: Dr. Maria John Newton Amaldoss, Australian Centre for Nanomedicine, UNSW Sydney, Sydney, NSW 2052, Australia, tel: +61426236587; e-mail: dramjnewton@gmail.com, m.amaldoss@unsw.edu.au
Imtiyaz Ahmed Najar, Swift School of Pharmacy Rajpura, Punjab, India, +917889393332; e-mail: najarimtiyaz1992@gmail.com

This article is available in open access under Creative Common Attribution-Non-Commercial-No Derivatives 4.0 International (CC BY-NC-ND 4.0) license, allowing to download articles and share them with others as long as they credit the authors and the publisher, but without permission to change them in any way or use them commercially

available, which are not providing the successful maintenance of the remission, therefore advanced drug treatments through the drug delivery systems are highly recommended [5]. IBD disease occurs in the genetically susceptible individual due to the dysbiosis of their microbiota caused by the abnormal immune response [6]. The significant number of evidences confirms the role of microbiota in IBD. Inflamed mucosa demonstrates the reduced diversity in mucosa-associated bacteria with the notable decrease in *Bacteroides* and *Firmicutes*, which is associated with anti-inflammatory properties and increase in *Enterobacteriaceae*, *Escherichia coli* and *Fusobacterium* [7–11]. This changes in microbiota are termed as “dysbiosis” [7–9].

Antibiotics have the potential to alter the composition of the gut microflora by promoting beneficial bacteria [10, 11]. Antibiotics also reduce the activity of bacterial enzymes and demonstrate the direct correlation between activity reduction and clinical response. In IBD, antibiotics play a significant role to reduce the effect of harmful pathogens by penetrating intracellular locations where the microorganisms are embedded within [12]. Further, Antibiotics also demonstrates direct immunomodulatory [13–15] and anti-inflammatory properties [16, 17]. As a gastrointestinal antibiotic rifaximin demonstrates significant immunomodulatory and anti-inflammatory properties [18, 19]. Rifaximin is a potential alternative to the other therapeutic agents which cannot pass through the walls of GIT to enter the systemic circulation [20]. Rifaximin, a non-systemic gastrointestinal antibiotic has broad-spectrum antimicrobial potential, increased faecal concentration, and low systemic absorption makes this drug as a suitable agent for gastrointestinal disease [21, 22]. The primary mechanism of action of rifaximin involves the inhibition of bacterial RNA and the maintenance of microfloral balance. Other studies have also shown rifaximin to be a pregnane-X receptor (PXR) activator [11]. As PXR is responsible for inhibiting the pro-inflammatory transcription factor NF-kappa B (NF-κB) and is inhibited in IBD. Rifaximin is highly effective than other antibiotics in IBD and induced remission of moderately active Crohns disease in 2/3 of the treated subject moreover, the effectiveness of rifaximin in human IBD and experimental colitis was reported in many kinds of literature [23–25]. Rifaximin was examined on the moderately ac-

tive Crohn's disease patients in multicentre, double-blind, placebo-controlled, varying dose study which revealed that administration of 800 mg rifaximin for twice daily for 12 weeks induced remission with few adverse events [24–26]. In the study by Pantera et al. by using an extended intestinal release formulation revealed that there are several potential unknown mechanisms by which the antibiotic alter the disease patterns of IBD [27].

Due to the lack of polysaccharides degrading enzymes in the human body most of the polysaccharides are indigestible in the GIT however they undergo chemical and structural modification by the enzymes, salt and pH of GIT [28] instead they are fermented by the microbiota enzymes present in the large intestine to produce short-chain fatty acids [29]. Tamarind gum polysaccharide (TGP) is a natural polysaccharide derived from the seeds of *Tamarindus indica* L.A. Being a polysaccharide with non-degradability in upper GIT, TGP can carry the loaded drug to the colon without releasing the drugs in the upper GIT and serves as the colon targeted drug delivery system [30–32]. TGP is gaining acceptance in the pharmaceutical and cosmetics industries. TGP demonstrates the high drug loading capacity, increased swelling index, mucoadhesive property and high thermal stability. Due to these properties, TGP is widely used as a stabilizer, thickener, binder, release retardant, modifier, suspending agent, viscosity enhancer, and emulsifying agent [33]. The recent works also shown the use of TGP as oral, buccal, colon, ocular and nano drug delivery systems [34].

Nanoparticles have an advantage over the conventional dosage forms in terms of specificity and reduced dose. The nanoparticles fabricated by the polysaccharides demonstrated the potential to target the drugs to the colon. The nature of the microbiota changes not only through the GIT but also changes cross-sectionally on the mucosal surface moreover; bacteria spread over the lumen and epithelial cells by adhering to the mucosa [35]. Studies suggest that since the bacteria occupy the lumen, epithelial cells, and mucosa delivering the rifaximin as a nanoparticles form with the mucoadhesive polymer such as TGP enhances the therapeutic efficacy in IBD. Occasionally, certain pathogens such as *Shigella*, *Salmonella*, and *Campylobacter* can invade the mucosal surface and causes enteric infections. *Salmonella* and *Campylobacter* have been suggested to play an aetiological role in the de-

velopment of IBD [36]. Rifaximin in the form of nanoparticles is the right choice to treat these IBD causing pathogen as nanoparticles can penetrate the mucosa and cell more efficiently and kills the internalized pathogens.

In this research work, we have developed a microflora activated natural polymer-based tamarind gum nanoparticles (TGN) loaded with rifaximin. Since the tamarind gum is mucoadhesive, which may adhere to the colonic mucous and stay an extended period to release the drug. Developed nanoparticles were characterized for hydrodynamic size, zeta potential by photon correlation spectroscopy and transmission electron microscopy (TEM). The nanoparticles were tested for the drug loading and drug release profile and release kinetics. The best formulation was selected based on the characterization, drug loading and drug release profile and subjected to therapeutic efficacy studies. The selected best formulation was used for the therapeutic efficacy study in TNBS induced IBD model rats. The colon profile, and biochemical parameters such as SOD, GSH, MDA, MPO and TNF- α were reported. The section of the colon was subjected to histopathological studies. The results of the therapeutic efficacy demonstrated that the developed formulation has significant therapeutic potential in TNBS induced IBD model rats. The study results revealed that rifaximin loaded tamarind gum nanoparticles have substantial therapeutic potential as compared to the standard IBD drug (mesalamine).

Materials and methods

Animals

Male Wistar rats (180–200 g) were obtained from Venus Remedies Animal House, Baddi (H.P). Animals were housed in polypropylene cages under the controlled environmental condition in terms of temperature ($23 \pm 2^\circ\text{C}$), humidity (50–70%), 12/12 h light/dark cycle and fed with standard rodent diet (M/s Ashirwad Industry, Mohali, India).

Chemicals

Rifaximin — Zhejiang Sixian Pharmaceutical Co. Ltd., tamarind gum, PEG 400 — Central Drug House (P) Ltd., New Delhi, Span 80 — Central Drug House (P) Ltd., New Delhi, Acetonitrile Central Drug House (P) Ltd., New Delhi, Dichloromethane — Central Drug House (P) Ltd., New Del-

hi, Glutaraldehyde 25% solution — Central Drug House (P) Ltd., New Delhi, acetic acid glacial — Central Drug House (P) Ltd., New Delhi. Na_2HPO_4 (dibasic) sodium phosphate NaH_2PO_4 , (monobasic) sodium phosphate — A.B. Enterprises Mumbai, EDTA — Loba Chemie Pvt. Ltd., Mumbai, TNBS (2,4,6 trinitrobenzene sulphonic acid) — Sigma Aldrich, Mumbai, carboxy methyl cellulose — S.D. Pharmaceutical, ethanol — Indian Chemical Company, Delhi, diethyl ether — A.B. Enterprises, Mumbai, TBA and DMSO reagents were purchased from Hi-Media Lab Pvt. Ltd., sodium nitropruside, sodium cyanide and sodium carbonate were purchased from Sisco Research Laboratory, Mumbai, glutathione from Hi-Media Lab Pvt. Ltd.

Fabrication of tamarind gum loaded rifaximin nanoparticles

Nanoparticles were prepared by using o/w emulsion polymer cross-linking technique. The aqueous phase was prepared by dissolving TGP in Milli-Q water in the concentration of 0.2% (w/v) and kept aside for saturation. TGP aqueous phase was subjected to bath sonication to dissolve the undissolved gum. 20 mL of the aqueous phase was kept under homogenizer at 1000 RPM. 10 mg of rifaximin was dissolved separately in 5 mL of dichloromethane. Rifaximin was added dropwise with the help of a needle in tamarind gum solution during continuous stirring. Span 80 (4 mL) was added dropwise under the stirring conditions, and a few minutes later, 10 mL of glycerol was added, which acts as a stabilizer in the aqueous phase. Finally, distilled water was added (10 mL), which destabilizes the equilibrium. Nanoemulsion was formed after rotating for 10 minutes at constant 1000 RPM. Crosslinking agent glutaraldehyde (25%) 2ml was added slowly to the system at this stage under continuous stirring to effect cross-linking of the TGP and rifaximin. Cross-linked nanoparticles as collected by subjecting to centrifugation. The prepared nanoparticles were collected and tested for morphological characteristics.

Characterization and evaluation of rifaximin polymeric nanoparticles Fourier transformed infrared (FTIR) spectroscopy analysis

FTIR Spectra of the rifaximin alone and physical mixtures of RFX and polymer and excipients

were recorded by using a Perkin Elmer (USA), from 4000–400 as scanning range between wavenumber (cm^{-1}) and % transmittance. Samples were prepared in KBr discs (2 mg sample in 200 mg KBr) with the hydrostatic press at the force of 5 cm^{-2} . Experiments were duplicated to check the reproducibility. The major sharp and significant peaks (functional groups) of the drug, drug and excipient mixture and drug loaded nanoparticles were analysed.

Particle size and zeta potential

The mean diameter of RFX nanoparticles in the dispersion was determined by (PCS) (Delsa NanoTM Common; Beckman Coulter) at an angle of 90° [37]. The prepared nanoparticles were dispersed in the milliQ water and sonicated for 3 min. Later the nanoparticles dispersion is transferred to the zeta sizer shell and measured for the hydrodynamic size. Nanoparticles were characterized for distribution width (D_{10} , D_{50} and D_{90}), mean particle size, span and polydispersity index. The values were reported in triplicate with mean diameter \pm standard deviation. Zeta potential was also measured by using zeta sizer (Delsa NanoTMC; Beckman Coulter) under the same conditions except the samples were kept in low conductivity zeta cell to meet the instrumental requirements.

Transmission electron microscopy (TEM)

TEM was used to characterize the morphology of RFX loaded nanoparticles. Nanoparticles were appropriately suspended with distilled water HPLC grade and subjected to sonication for 2 minutes. A drop of prepared nanoparticles formulation was placed on the carbon-coated copper grid and allowed to dry overnight. The superfluous was wiped out with Whatman filter paper, and TEM images were obtained by using (HITACHI Japan, Model H7500 ID).

Drug entrapment efficiency

10 mL of RFX nano dispersion was subjected to entrapment efficiency test to check the percentage of incorporated rifaximin. Entrapment efficiency was determined spectrophotometrically at 293.6 nm using systronics 2201 UV spectrophotometer. Previously 10ml of nanosuspension was prepared and subjected to centrifugation at 5000 RPM for 45 minutes. The supernatant was separated and subjected to spectrophotometric measurement

to determine the unloaded drug. The amount of free drug was detected in the supernatant, and the amount of loaded drug was selected as a result.

Drug release profile of rifaximin nanoparticles

The drug release pattern of the nanoparticle formulations was determined by using a dialysis bag (Himedia labs, cut off weight 12000–14000 Da) method for 12 h. The dialysis bag was soaked in MilliQ water for 12 hours before use. Later the bag was tied with the help of a thread in one side of the open-ended cylinder. The amount equivalent to 10 mg of RFX containing nanosuspension was introduced into the dialysis bag. The bag was placed in the beaker containing 100ml of the receptor compartment with media mimicking pH conditions of the GIT. The media simulating colonic pH conditions were prepared with rat cecal contents in order. The system was kept under stirring magnetic needs at 100RPM. In this setup dialysis bag with a cut-off of 12000-14000 Da retains the nanoparticles and allows the free drug to pass through. The dissolution samples were collected at predetermined time intervals of 0, 0.5, 1, 1.5, 2, 3, 4, 5, 6, 7, 8, 12 h and were replenished with the fresh media to maintain sink conditions. The samples were analysed spectrophotometrically by using UV spectrophotometer (Systronics; 2201, Gujrat) against the blank. All the observations were carried out in triplicate. (Yadav and Mishra, 2012), (Patel and Parikh, 2013).

Procedure for preparation of rat cecal contents medium dissolution

Before carrying out the study on animals, the study protocol was scrutinized by an institutional animal ethical committee (IAEC) and approved. The final stage of dissolution study was performed in the media containing rat cecal content to assess the effect of enzymatic activity of the colonic bacteria on nanoparticles. The cecal samples were collected from five Wistar rats weighing 240–400 grams. Rats were maintained in normal diet conditions, but 1ml of 2% w/v of pectin dispersion administered orally with a Teflon cannula for seven days. The pectin dispersion induces the colonic enzymes so that the cecal content was enriched with the polysaccharide digesting enzymes. The rats were sacrificed 45 minutes before the drug release studies their abdomen was cut open to collect the

rat caecal contents. The caecal contents of the animals were pooled up, and the final 4% w/v caecal dilution was prepared. The 4% caecal contents were introduced into the dissolution media after the 5th hour of the study continued up to 12 h. The samples were analyzed by UV spectrophotometer. The withdrawn sample was replaced with the fresh media bubbled with carbon dioxide to maintain sink conditions. The withdrawn samples were diluted and centrifuged to separate solid contents. The supernatant liquid was collected and filtered through the bacteria proof filter, and the filtrate was analyzed for RFX contents using double beam UV spectrophotometer wavelength of 330–332 nm.

Therapeutic efficacy study of nanoparticles

Experimental design

The animal study protocol was approved by the Institution Animals Ethics Committee (IAEC) (SSP/IAEC/17/03). The rats were randomly assigned into five groups (n = 5). The vehicle and test items were administered to the respective group for ten days after TNBS induction to till completion of the study. Group 1, is a control group administered with the PBS instead of TNBS. Group 2 is colitis group received TNBS by intracolonic administration. Group 3 is a reference drug group received a drug Mesalamine (50 mg/kg body weight). Group 4 is the nanoparticles treatment group. TNBS colitis was induced as per the original method developed by Morris et al. [38] briefly; rats were fasted for 24 hours and allowed free access to water. Animals were anaesthetized with chloral hydrate (300 mg/kg intraperitoneal). Rats were administered with TNBS (50 mg/kg) dissolved in 50% ethanol by inserting a Teflon cannula (2 mm) 8 cm through the anus so that the tip advanced to the descending colon. Rats were kept in a head-down position for 1 min to prevent leakage for the intracolonic distillate, and the rats were kept in warm condition until regaining consciousness. The control group is administered with the PBS instead of TNBS.

The nanoparticles were administered through the oral route by using a gavage needle attached to a graduated syringe. The dose-volume was adjusted according to the bodyweight of the individual animal.

Rifaximin nanoparticle group (TGN1) received a freshly prepared rifaximin NP as a suspension in

0.5% w/v Carboxymethyl cellulose (CMC). Group 3 was administered with reference drug mesalamine. The volume of the Mesalamine administrated dose was 10 mL/kg body weight (50 mg⁻¹/kg) by the oral route. Rifaximin dose (1 mg kg⁻¹ /day) was given as a suspension in 0.5% w/v Carboxymethyl cellulose (CMC), p.o., once a day, in the morning. The TNBS groups received a TGN1 for 11 consecutive [39].

Body weight

Animals were observed for general clinical signs once daily on all days throughout the study duration. Bodyweight of animals was recorded before the initiation of treatment and after that weekly once during the course of the study and before the termination of the study. The body weight, water and food consumption were recorded daily throughout the experiment.

Haematology

Blood was collected by retro-orbital plexus puncture on day 14 in centrifuge tubes for serum separation. The serum was separated by centrifugation of blood at 3200 rpm for 10 minutes and stored at -20°C until analysis. The blood was collected into plain capped bottles containing ethylene diamine tetraacetate (EDTA) by a modified method [40]. The samples were immediately used for the estimation of the different parameters.

Microscopic, macroscopic and biochemical analysis

After the treatment period, the rats were euthanized by deep ether anaesthesia, and then laparotomy was performed. The distal 8 cm portion was excised and cut longitudinally then cleaned with ice-cold saline phosphate buffer to remove adherent adipose tissue and faecal matter. The colon was blotted gently to dry and weighed then macroscopic assessment was done. The portion of the distal colon was used for the histopathological, immunochemical and biochemical investigation. The colonic segments were considered, opened longitudinally and examined for damage. The colon was scored for macroscopically visible damages on a 0–10 scale by two observers unaware of the treatment, according to the criteria described by Bell et al. [41]. The macroscopic damage was used to assess the severity of the colonic injury. The representative colon specimen was taken from a region adjacent to

the gross, microscopic damage. Similarly, the specimen was collected from all the groups and fixed in 4% buffered formaldehyde and embedded in paraffin. Equivalent colonic segments were also obtained from the non-colitic group. Full-thickness sections of 5 μm were obtained at different levels and stained with hematoxylin and eosin.

The portion of tissue homogenate was used to analyze the biochemical assay. The colonic tissue segments were homogenized at 4°C in 2 mL of ice-cold saline with a glass homogenizer, and the homogenate was passed through a cellulose filter to remove impurities and divided into aliquots for biochemical analysis. Colonic GSH levels were determined by the method described by Beutler et al. [42] in which 5,5'-dithiobis 2-nitrobenzoic acid (DTNB) used as a reagent. The absorbance of the colour development measured at 412 nm and expressed in nmol/g tissue. The lipid peroxide level is expressed as malondialdehyde (MDA) according to the thiobarbituric acid assay of Buege and Aust [43]. The absorbance was measured at 535 nm, and the results were expressed as nmol/g tissue. The total NO was determined by the method developed by Miranda et al. [44] (measuring the metabolites, especially nitrite (NO_2^-) and nitrate (NO_3^-).

The absorbance was measured at 540 nm, and the expressed as nmol/g tissue. MPO is a marker for the neutrophil infiltration, was estimated according to the method developed by Krawisz et al. [45] with the minor modification. One unit of MPO activity is defined. The activity of MPO, a marker for neutrophil infiltration, was estimated according to the method of with slight modifications. One unit of MPO activity is defined as the amount of enzyme converting 1 μmol of H_2O_2 to water in 1 min at 25°C. and the absorbance was measured at 460 nm for 4 min. Levels of TNF- α in colon homogenate supernatants were measured using ELISA kits. All the procedures were performed

according to the manufacturer's instructions. The corresponding levels were expressed as pg/g wet tissue. The SOD activity of colon tissue was determined by superoxide dismutase as described by Fontana et al. [46]. The different concentrations of standards and samples were added and thoroughly mixed, and then the samples were incubated 5 min at room temperature. After incubation for 5 min at room temperature, the absorbance was measured at 562 nm against an appropriate blank solution. Colon tissue content of TNF- α was measured by ELISA assay according to the kit instruction and expressed as pg per mg protein.

Statistical analysis

The data were expressed as mean \pm S.E.M. Data was subjected to statistical analysis using ANOVA, followed by Dunnett's multi-comparison test to draw a comparison between treatment groups and TNBS control group. Any animal not responding either to FCA or to the treatment was excluded from the analysis. $p \leq 0.05$ was considered as statistically significant.

Results and discussion

Fabrication and characterization

Five different formulations (TGN1-TGN5) of tamarind gum nanoparticles were prepared by O/W Emulsion polymer cross-linking method (Tab. 1). The Tamarind gum concentration was decreasing from 500 mg to 250 mg, whereas the cross-linking agent glutaraldehyde concentration was increased from 2 to 4 mL. The formula containing a lower concentration of polymer is less likely to cross-link with the drug; therefore, a slightly higher concentration of cross-linking glutaraldehyde was added. The drug concentration was maintained at 10 mg in all the formulations the other ingredients such as span and glycerol also maintained as constant level

Table 1. Composition of tamarind gum (TGP) nanoparticles formulations

Formulations	Tamarind gum [mg]	Rifaximin [mg]	GTA [mL]	Span 80	Glycerol	Organic phase (Qty)
TGN1	500	10	2	4 mL	10	5ml
TGN2	450	10	2.5	4 mL	10	5ml
TGN3	350	10	3	4 mL	10	5ml
TGN4	300	10	3.5	4 mL	10	5ml
TGN5	250	10	4	4 mL	10	5ml

in all the formulations (Tab. 1). The nanoparticles were analyzed for characterization parameters such as mean diameter, polydispersity index, zeta potential and %EE. The best formulation was selected from master sizer analysis and then subjected to the characterization techniques such as TEM, zeta sizer and zeta potential. The drug release profile study was conducted to the three selected formulation (TGN1-TGN3). The best formulation (TGN1) selected from the characterization study was subjected to therapeutic efficacy study.

FTIR study

The FTIR results showed that there is no chemical interaction between the drug and used excipients/polymers, and no chemical modification occurred. The drug rifaximin showed the significant bands at 3434.35 cm^{-1} for OH stretch. C-N stretching was observed at 1159.39 cm^{-1} . The peak for ester linkages was observed at 1649.26 cm^{-1} , and pyrrole ring was marked at 1589.22 cm^{-1} . The peak representing OH bending was observed at 947.43 cm^{-1} . The rifaximin and PF68 demonstrated the distinct peak representing -OH stretching at 3464.16 cm^{-1} rifaximin, ester linkage at 1647.19 cm^{-1} , and C-N stretch and -OH bending was observed at 1111.1 cm^{-1} 960.8 cm^{-1} respective. This results indicated that PF68 was chemically compatible with the rifaximin. The tamarind gum and rifaximin mixture demonstrated the rifaximin peaks at -OH stretching at 3431.31 cm^{-1} , ester linkage at 1650.24 cm^{-1} and C-N stretch and -OH bending was observed at 1159.31 cm^{-1} 947.35 cm^{-1} respectively. This result confirms the chemical compatibility between tamarind gum and rifaximin. The rifaximin nanoparticles also subjected to FTIR analysis to examine any chemical interaction happened in the formulation. The final formulation of tamarind gum nanoparticles (TGNP) containing tamarind gum, glycerol, span 80 and glutaraldehyde shows significant peaks at 3392.3 cm^{-1} for OH group stretching, 1645.8 cm^{-1} for ester linkages, 1113.16 cm^{-1} for C-N stretching and 996.18 cm^{-1} for OH bending which rules out any interaction between the drug and used excipients in the nanoparticles formulation. The FTIR spectrum of the medicine with different excipients mixtures showed the drug is in its intact form in physical mixture as well as in the formulations. Moreover, the FTIR results of tamarind gum nanoparticles indicated that the rifaximin presence

in the nanoparticles with all the major peaks representing rifaximin (Fig. 1).

Optimization of particle size

The prepared five formulations were analyzed under master sizer for distribution width, mean particle size (MPS), SA (m^2/g), span and uniformity (Fig. 2). Among this TGN1, TGN2 and TGN3 were found to be the best formulation. The particle size analysis report of Master sizer was found to be varying with the formulations (TGN1-TGN5). The mean particle size among these formulations was found to be lowest in TGN5, i.e. 1115.4 and the TGN1 were reported with 1166.9 . The best formulation TGN1 was noted with 1166.9 . The value of the particle size of TGN1 was a bit higher as compared to TGN5. The formulations such as TGN1, TGN2, and TGN3 which were showing nano range in master sizer reports were further subjected to analysis by Delsa NanoTM C. Before going to an analysis by zeta sizer (Delsa NanoTM C) the formulations TGN1, TGN2, TGN3 were subjected to probe sonication for 3 minutes with an impulse of 5 seconds. The probe sonication leads to the reduction of particle size as well as improves the stability of the formulation. The results after the analysis by Delsa NanoTM C revealed that TGN1 could be declared as the best formulation in terms of size with a value of 228.8 ± 159.2 and the detailed zeta sizer analysis is discussed below.

Particle size analysis and zeta potential

The best formulations of tamarind gum group (TGN1-TGN5) were subjected to particle size analysis by Beckman Coulter. The initial master size analyzer indicated that the formulation TGN1, TGN2 and TGN3 were found to be in the lower nano-size range. Among the three tamarind gum formulations (TGN1, TGN2, TGN3) the formulation TGN1 the size of 171.4 nm , which is the lowest of all the other nanoparticles. The polydispersibility index of the formulation was found to be 0.277 for TGN1, and it was 0.203 and 0.256 respectively for TGN2 and TGN3. The mean particle size of the TGN1 was 228.8 ± 159.2 , and it was 304 ± 164.4 and 477.9 ± 324.7 for TGN2 and TGN3 respectively. Likewise D_{10} , D_{50} , D_{90} also demonstrated 75.60 , 179.60 , 429.80 respectively whereas TGN2 and TGN3 demonstrated the highest values which proved that TGN1 is found to be better nanopar-

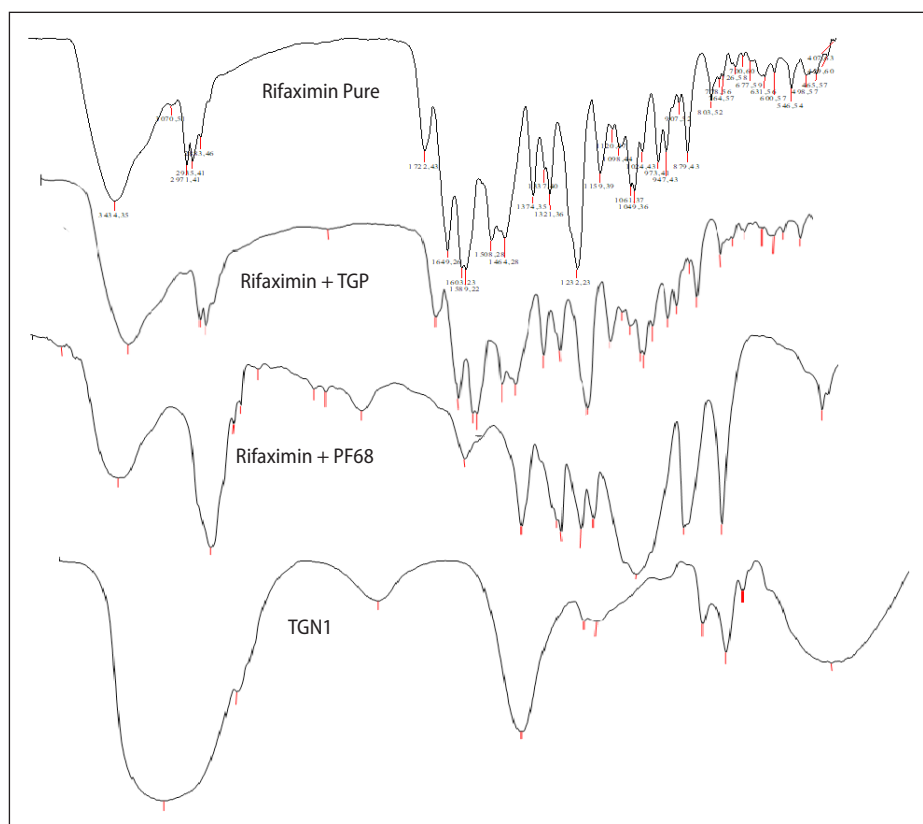


Figure 1. Overlay spectrum of Fourier transformed infrared (FTIR)

ticle formulations which contain tamarind gum 0.5%, glutaraldehyde 2 mL and span 80 4 mL and glycerol 10 mL (Fig. 3A-C).

The best formulation of TGN1 was tested for zeta potential. The zeta potential of the nanoparticles is essential to know the surface charge of the nanoparticles. The particle surface charge value indicates the stability of formulation at the macroscopic level. A minimum zeta potential of ± 30 mV is required for electrostatically stabilized preparation and a minimum of ± 20 mV for steric stabilization. The zeta potential values are commonly calculated by determining the particle's electrophoretic mobility and then converting the electrophoretic mobility to the zeta potential. Zeta potential is the indicator of the stability of the prepared nanoparticles; it is a necessary test. The zeta potential of the tamarind gum (TGN1) nanoparticles was found to be -26.44 mV, and it is found to be satisfactory for maintaining stability (Fig. 3D).

Transmission electron microscopy (TEM)

The microscopical analysis of prepared tamarind gum nanoparticles formulation (TGN1) was

done by using TEM. The particles were found to be spherical and also demonstrated that the particles appear in the uniform size range (10–40 nm), which was studied from the figures taken at various magnification 200000X-3000000X. The particle size determination in the TEM images was found to be 19 nm, 29.1 nm, 32.9 nm, and 32.6 nm revealed that particles had a narrow size distribution range (Fig. 4).

Percentage of entrapment efficiency

The highest percentage of entrapment efficiency was found to be within TGN1 ($85\% \pm 2.71$). This revealed that the lowest particle size encouraged the highest entrapment efficiency. The other formulations were also demonstrated the entrapment efficiency of $75\% \pm 5.19$, $72\% \pm 4.72$ respectively for TGN2 and TGN3.

In vitro drug release and release kinetics

All the formulations (TGN1-TGN5) were subjected to drug release time profile study (Fig. 5). *In vitro*, drug release studies were performed by using the various buffers such as 0.1N HCl (1.2 pH), 6.8

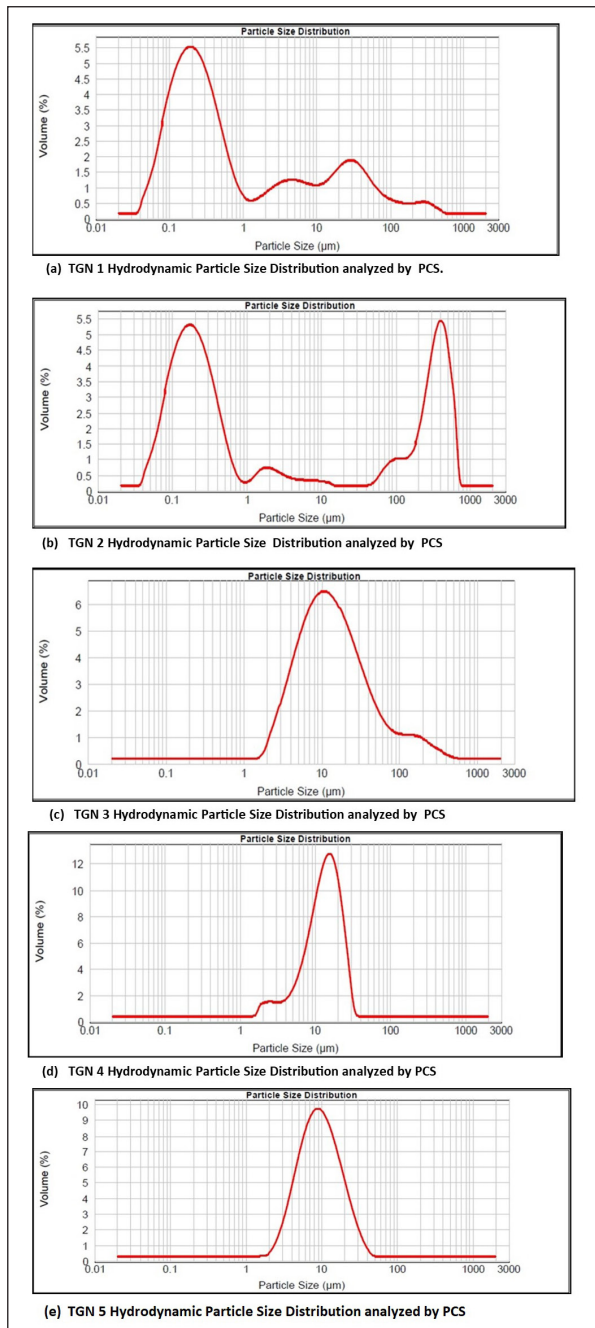


Figure 2. Optimization of hydrodynamic particles size (TGN1–TGN5)

phosphate buffer and 7.4 phosphate buffer to mimic the GI conditions of stomach, intestine and colon respectively. Drug release studies were performed up to 12 h. The samples were taken at various time intervals. During the acidic conditions (1.2 pH), the samples were withdrawn for every half an hour up to 1.5 h, which is also simulating the GI transit time. Then during the intestinal conditions (6.8 pH) the samples were withdrawn for every 1h up

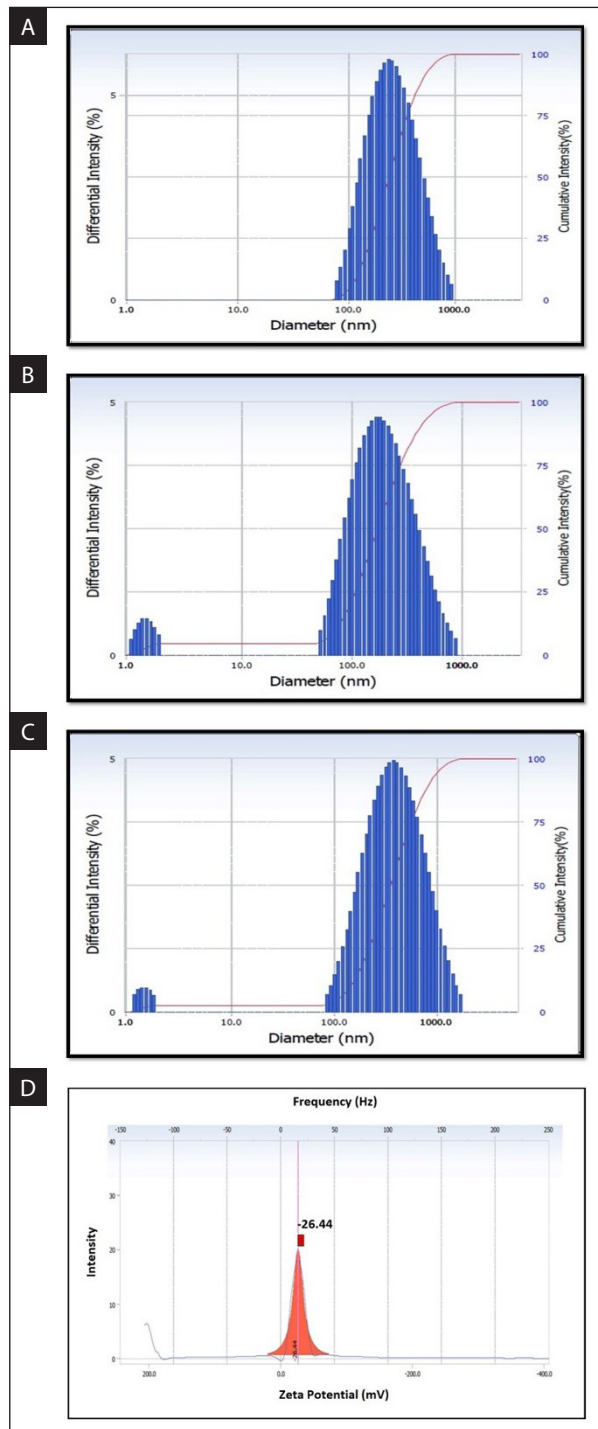


Figure 3. Particle size analysis and zeta potential of selected best formulations (TGN1-TGN3). **A.** Hydrodynamic size distribution of TGN1. **B.** Hydrodynamic size distribution of TGN2. **C.** Hydrodynamic size distribution of TGN3. **D.** Zeta potential of TGN1

to 5h followed by the colonic diseases 7.4 pH the samples were withdrawn at every 1 h up to 8 h then two samples were taken in 10 h and 12 h. After every withdrawal of the samples, the system was

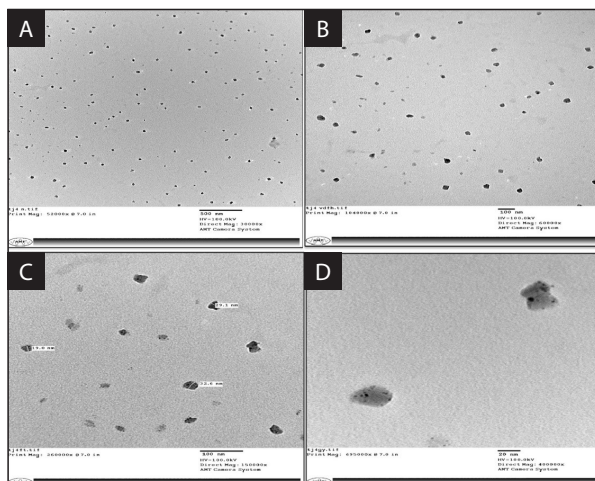


Figure 4. TEM images of TGN1 shows images in different magnification (A) TGN1 imaged at 30,000X magnification shows the uniformity of the nanoparticles in TEM imaging (B) TGN1 imaged at 60000X magnification (C) TGN1 imaged at 150000X, demonstrated the size of the nanoparticles in 19.0 nm, 32.6 nm and 29.1 nm (D) TGN1 imaged at 400000X and shows the individual TGP nanoparticles the contrast point inside the nanoparticles indicated the drug loading of rifaximin

replenished with fresh media. The formulation TGN1 was found to be best in controlling the drug for colonic delivery. During the acidic condition, the formulation TGN1 released only 19% of the drug at 1.5 h, being a colon targeted nanoparticles the formulation must release significantly less amount of medicine in the upper GI tract, demonstrated in the prepared tamarind gum nanoparticles of TGN1. TGN1 released 10% of the drug at the end 1.5 h simulating acidic condition whereas TGN2 and TGN3 released 16 and 19% respectively which indicated the that the TGN1 is better in controlling the drug release in the acidic environment. Rifaximin is cross-linked with the tamarind gum, and there is no enzyme available in the upper GI tract to digest the tamarind gum polysaccharides and release the drug. Since the TGN1 contains the tamarind gum concentration at the highest, which might have influenced the drug release, there is no high difference in the overall release pattern of the three formulations however based on the characterization techniques and controlling the drug release in the upper GI tract, TGN1 can be considered as the best formulation. The drug release time profile of formulations was studied by fitting with the various equations such as Zero order, First order, Higuchi, Korsmeyer Peppas and Hixon Crowell.

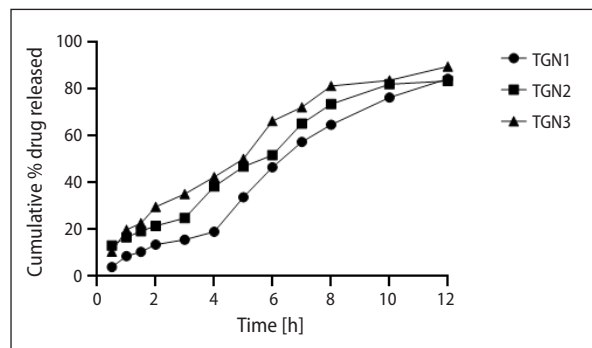


Figure 5. Cumulative percentage of drug release of TGN1-TGN3

The formulations TGN1-TGN3 demonstrated the best fit with Zero order. Kinetics model. The best formulation TGN1 demonstrated the R^2 value of 0.994. The mechanism of the drug release was analyzed by using Korsmeyer-Peppas exponent “n” to characterize different release mechanisms. The best formulation demonstrated the “n” value of 0.499, which is in between the range of $0.45 < n < 0.89$ indicates non-fickian anomalous diffusion. The analysis of drug release mechanism confirmed that formulation follows non-fickian or anomalous diffusion which confirmed controlled as a drug release mechanism.

Therapeutic efficacy of tamarind gum-rifaximin nanoparticles

Body weight and colon profile

The fabricated tamarind gum nanoparticles (TGN1) for oral delivery was assessed for their therapeutic efficacy in improving TNBS induced colitis in Wistar rats. To determine the severity of colitis, the clinical signs such as body weight loss, diarrhoea and rectal bleeding were noted. The rats induced with TNBS shown significant weight loss (Fig. 6A). The animals also revealed the high ulcer index score accompanied by diarrhoea and rectal bleeding. The rats also demonstrated the substantial changes in colon weight/length ratio, which is a reliable marker of colon inflammation [47]. The macroscopic examination of colon revealed severe colonic injury characterized by mucosal damage, thickening of the bowel wall, hyperemia and oedema after the administration of TNBS. The observation on TNBS control group revealed the significant intestinal wall thickening, well-established ulcer scores and associated with ulcer area that is larger

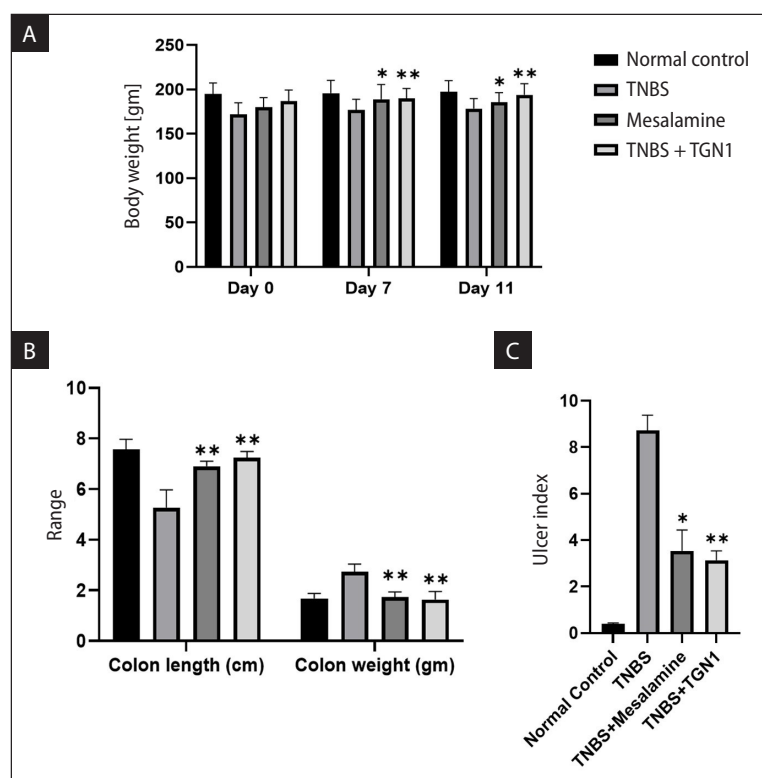


Figure 6. A. Animal body weight profile; B. Ulcer index; C. Colon profile. Values as expressed as Mean \pm SEM; n = 5 animal/group value are expressed as mean \pm SEM; n = 5 animals/group. *p < 0.05 significant different from TNBS colitis by one-way ANOVA

around 2 cm were noted in TNBS group [48]. The TGN formulation reduced the colitis significantly against the TNBS control group. The ulcer index of TNBS group (8.98 ± 0.69) indicated the significant difference from the control group (0.34 ± 0.13). The ulcer index of the TGN and Mesalamine group was significantly less than the TNBS group, which indicated the fair recovery from diseases colonic conditions (Fig. 6B–C).

Haematology

The haematological parameters in serum provide information about the inflammatory conditions of the colon. The haematological parameters of the TNBS group are significantly (*p < 0.05) different from the control group (Fig. 7A). The haematological parameters of the TGN group have shown significant improvement (*p < 0.05) as compared to the TNBS group. Many kinds of the literature revealed a substantial increase in the platelet count associated with IBD conditions [48–50]. Moreover, in human IBD is reported with 50–70% increase in circulating platelet count [51]. The platelet level was increased in the TNBS animal group, and normal

and treatment groups are not demonstrating the significant increase in platelet levels (Fig. 7B). The various component in the blood remained stable in TGN1 group as well as in the Mesalamine group. Monocyte, polymorphonuclear and endothelial cells are playing a significant role in the inflammatory progress [52]. The activation of these components causes the respiratory burst and causes the infiltration into tissues and increases oxidative stress through the pro-inflammatory agents and ROS. The pathological mucosal damages are induced majorly by the influence of the ROS level. This will intern reflected by the ROS metabolites such as SOD, GSH and MDA [53].

Biochemical parameters

All the animals were sacrificed, and biochemical parameters such as GSH and MDA were determined to assess the inflammation. SOD and GSH act as primary scavengers of free radical which protect cellular enzymes [54]. Superoxide dismutase (SOD) plays a significant role in antioxidant activity in the protection of cells, against the oxidative damage [55]. The predominant part

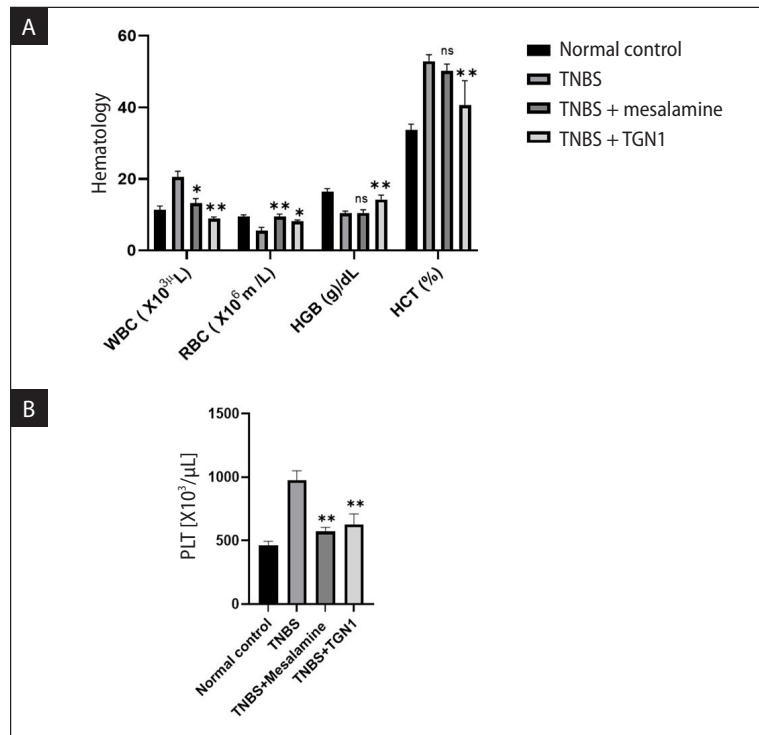


Figure 7. A. Haematological profile; B. Platelet profile. Values as expressed as mean \pm SEM; n = 5 animal/group. Value are expressed as mean \pm SEM; n = 5 animals/group. *p < 0.05 significant different from control group, #p < 0.05 significant different from TNBS colitis by one-way ANOVA

of SOD is to detoxify superoxide anion to H_2O_2 [56]. Then, the CAT and the GSH -Px enzymes convert H_2O_2 into H_2O to protect the cells from ROS injury [57]. Overall the SOD levels are higher in the IBD pathogenesis due to their function of safeguarding the intestinal tissues from oxidative stress [58]. The highly toxic ROS dominates the defence mechanism and causes the intestinal injury and Glutathione SH (GSH) plays a significant role in the intracellular defence against oxidative stress which is essential for both functional and structural integrity of the GUT. GSH levels are depleted in inflammatory conditions, and this leads to the degradation of colonic mucosa, diarrhoea and loss of body weight [59–61]. The significant reduction in the glutathione content is a significant marker of colonic injury. The GSH levels of TNBS control group (0.598 ± 0.214) is significantly (*p < 0.05) higher than the control group. Mesalamine group and TGN group shown a significant difference from the TNBS group. Increased GSH level indicates the standard conditions of the colon and the recovery of the inflammatory conditions which are noted in the mesalamine and TGN group.

Myeloperoxidase is a lysosomal protein released into the phagosomes of neutrophils which reacts with hydrogen peroxide to form hypochlorous acid and tyrosine to form tyrosyl radicals which are highly cytotoxic [62]. Myeloperoxidase is often overexpressed in numerous inflammatory diseases, including IBD [63, 64]. The increased MPO activity was associated with initial neutrophil and later mononuclear cell infiltration [65]. The TNBS induced colitis causes the protonation and induced the infiltration of neutrophils in the colonic inflamed tissues [66]. MPO indicates the level of infiltration of neutrophils in the colon, which is usually higher in the colitic conditions. MPO itself possess cytokine-like properties and activates the neutrophils, which causes the release of a range of inflammatory mediators and ROS species [67]. The reduction of MPO level causes the reduction of neutrophil infiltration is the indicator of the inflammatory recovery [68]. Leukocyte infiltration was determined by biochemical analysis. In normal control, the leukocyte infiltration was significantly less due to the reduced MPO activity. However, in the TNBS group, the MPO activity was significantly increased (*p < 0.05) as compared to the normal

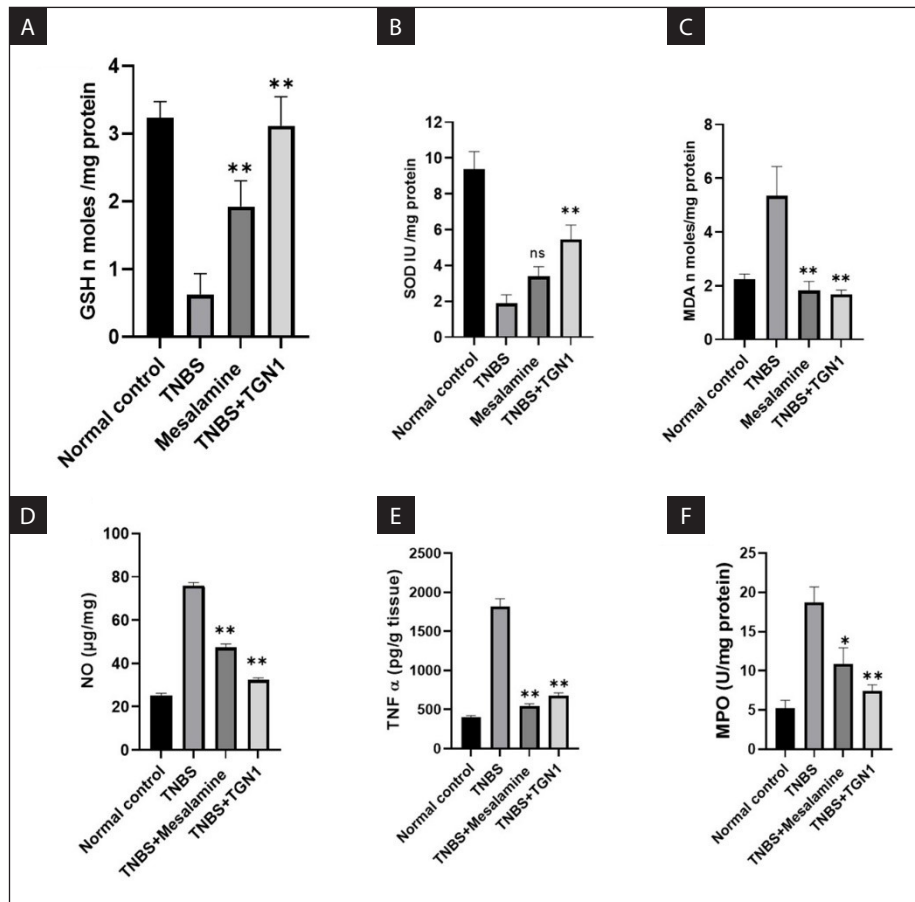


Figure 8. Biochemical analysis of colon lysate. **A–C.** Effect of TGN1 on (A), GSH (B), SOD (C), MDA in colon lysate of TNBS-induced Wistar rats; **D.** Effect of TGN1 on NO in colon lysate of TNBS-induced Wistar rats; **E.** Effect of TGN1 on TNF α in colon lysate of TNBS-induced Wistar rats; **F.** Effect of TGN1 in on MPO colon lysate of TNBS-induced Wistar rats. Value are expressed as mean \pm SEM; n = 5 animals/group.*p < 0.05 significantly different from TNBS colitis by one-way ANOVA

control group. The TGN treated group have shown the significant ($p < 0.05$) downregulation of MPO activity as compared to TNBS group. This is similar to the report of Fiorucci et al. [69] who administered rifaximin (30 or 50 mg/kg/day) to colitic mice which increased survival rates, reduced colitis severity, decreased colonic IL-2, IL-12, IFN- γ and TNF- α levels, and MPO activity Figure 8 shown the results of the NO, MPO, TNF- α , GSH SOD and MDA.

In mucosal inflammation, intestinal epithelial cells, neutrophils and macrophages produce the superoxide and nitric oxide. Superoxide and nitric oxide are formed by activating NDAPH oxidase and inducible nitric oxide synthase (iNOS) both are induced by inflammatory cytokines and more reactive oxygen, and nitrogen species are created through the NADPH oxidase and iNOS activation [70]. Rifaximin plays a role in regulating cytokine

expression, which is considered as an additional therapeutic effect on IBD condition independently of antibiotic effect. Rifaximin is a gut-specific ligand for the human nuclear receptor subfamily 1, group 1 member (pregnane-X receptor) which regulate cytokines expression [71]. iNOS is playing a significant role in the pathophysiology of inflammation, and NO reacts with ROS and acts as an oxidative agent. This causes the elevated level of ROS, which can damage the cytoskeleton of proteins and alters the tight junctions of epithelial permeability in intestinal epithelial cells and causes the barrier disruption [72, 73]. This process initiates IBD inflammation. The continuous increase of NO and superoxide level causes the production of highly toxic peroxynitrite which is believed to play the predominant role in colonic inflammation. The increased NO level causes the colonic tissue toxicity and mucosal damage. The

NO levels in the TNBS is significantly $*p < 0.05$ increased and indicating the increased inflammatory conditions whereas in the mesalmine group and TGN treatment group demonstrated significant potential to down regulated the NO level through the anti-inflammatory effect. Mesalmine has been known for reducing the NO toxicity level in the IBD similarly the rifaximin has the remarkable potential to reduce the NO toxicity.

TNF- α , the pro-inflammatory cytokines, play a significant role in the migration of NF- κ B into the nucleus and damages the cells. TNF- α involves the conscription of neutrophils and the inflamed colonic mucosa and initiates the inflammatory pathogenesis [37–40]. Chen et al. analyzed the role of rifaximin in mRNA expression of NF- κ B-regulated pro-inflammatory mediators in colonic tissues of mice. The treatment with rifaximin blocked the pro-inflammatory induction mediators. The rifaximin treatment inhibited the TNF- α -induced NF- κ B activity, thus helped the recovery of the colonic damage. Therefore the mechanism of action of rifaximin revealed the potential to antagonize the effects of TNF- α on intestinal epithelial through the inhibition of NF- κ B-mediated pro-inflammatory mediators by activating pregnane-X receptor, which induces detoxification genes. Sartor et al. [74] reviewed the mechanism of action of rifaximin and revealed that rifaximin plays a role more than the non-systemic bactericidal antibiotic and therapeutically work beyond inducing the remission.

The results showed a significantly higher expression of TNF- α concentration after the administration TNBS. The TNBS administration is known to increase TNF- α and IL-1 β and NF- κ B, which were found to be associated with the increased colonic injury [75, 76]. The increased expression of pro-inflammatory cytokines such TNF- α was significantly increased in the TNBS group as compared to the treatment and control group. The monocytes and macrophages initially activate the pro-inflammatory cytokines, including TNF- α . They play a significant role in the mucosal inflammation and immunity as well as involved in the many cellular processes such as metabolism, inflammation and apoptotic cell death [74]. The higher expression of TNF α levels in treatment and Mesalamine group significantly decreased as compared to the TNBS group, which

indicates the recovery of colonic inflammatory conditions [65]. The study results demonstrated the significant reduction in the TNF- α level in the TGN, and mesalamine treated rats hence proved the anti-inflammatory effect produced by the nanoparticles through a similar mechanism. A similar effect of reduced TNF- α level was reported with rifaximin (50 mg/kg/day), which significantly accelerates recovery in mice with established colitis [69].

Histopathological observations

Intrarectal administration of TNBS triggered the weight loss, bloody diarrhoea, rectal prolapse, and considerable bowel wall thickening. Rifaximin significantly improved colon histology [39]. The assessment of control group demonstrated no disturbance in the standard architecture of the colon. The TNBS induced IBD group showed an increased clinical score with the increased production of the mucous in the inflamed colon as compared to the healthy group (Fig. 9). Severe transmural disruption in the architecture of colon was observed in the TNBS group and which is also accompanied by the very high microscopic score due to tissue injury. The tissue injury was evidenced with focal necrosis of mucus submucosa and loss of epithelium. There is also oedema, crypt abscess, diffused leucocyte infiltration and accumulation of neutrophils in the mucosal layers and few lymphocytes in the submucosa. The inflammation process involves crypt hyperplasia, dilation and moderate goblet cell depletion. The groups receiving the nanoparticles (TGN) demonstrated the decrease in the severity of the inflammation.

The study results showed that TGN has the potential to protect against the histopathological damages occurred in the colon. The significant reduction in the severity of disease was noted on day 17 this is 72 hours after the drug administration. After the treatment period, the ulcer areas were showing the sign of the formation of new epithelium. The transmural lesions and goblet cell depletion was reduced. The clear indication of mucin restoration was recorded along with the restructuring of normal mucosa, submucosa and muscularis mucosa was observed. The overall observation confirmed the restoration of colonic glands indicated the restoration of colonic histology and restoration of normal cell function.

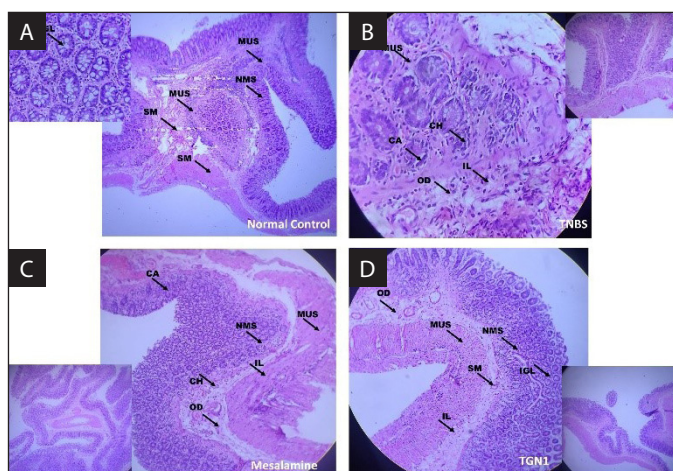


Figure 9. Tamarind gum–rifaximin nanoparticles on histopathology of TNBS-induced IBD model of Wistar rats. **A.** Normal control; **B.** TNBS control; **C.** Mesalamine treated group; **D.** TGN1 treated group. IGL — intestinal glands; NMS — normal mucosa; MUS — muscularis mucosa; SM — submucosa; OD — oedema; CA — crypt abscess; CH — crypt hyperplasia; IL — infiltration of leucocytes

Conclusion

In summary, the present study demonstrates that the rifaximin loaded tamarind gum nanoparticles can deliver the maximum amount of drugs at the colon. The nanoparticle formulations were stable with significantly high zeta potential. The best formulation TGN1 provided significant protection against the TNBS induced colitis in rats. The developed nanoparticles were able to ameliorate biochemical parameters as compared to the TNBS group. The TGN1 group shown the significant recovery in the histopathology, which is significantly equivalent to or higher than the reference drug mesalamine group and normal control group. Furthermore, these data support the overall improvement of inflammatory disease profile suggests that the rifaximin as oral nanoparticles delivery can improve the therapeutic potential of rifaximin drug in the IBD treatment.

Conflict of interest

None declared.

Funding

None declared.

References

- Huang Y, Chen Z. Inflammatory bowel disease related innate immunity and adaptive immunity. *Am J Transl Res.* 2016; 8(6): 2490–2497, indexed in Pubmed: [27398134](https://pubmed.ncbi.nlm.nih.gov/27398134/).
- Belkaid Y, Hand TW. Role of the microbiota in immunity and inflammation. *Cell.* 2014; 157(1): 121–141, doi: [10.1016/j.cell.2014.03.011](https://doi.org/10.1016/j.cell.2014.03.011), indexed in Pubmed: [24679531](https://pubmed.ncbi.nlm.nih.gov/24679531/).
- Matricon J, Barnich N, Ardid D. Immunopathogenesis of inflammatory bowel disease. *Self Nonself.* 2010; 1(4): 299–309, doi: [10.4161/self.1.4.13560](https://doi.org/10.4161/self.1.4.13560), indexed in Pubmed: [21487504](https://pubmed.ncbi.nlm.nih.gov/21487504/).
- Currò D, Pugliese D, Armuzzi A. Frontiers in Drug Research and Development for Inflammatory Bowel Disease. *Front Pharmacol.* 2017; 8: 400, doi: [10.3389/fphar.2017.00400](https://doi.org/10.3389/fphar.2017.00400), indexed in Pubmed: [28690543](https://pubmed.ncbi.nlm.nih.gov/28690543/).
- Kumar J, Newton AJ. IBD Modern Concepts, Nano Drug Delivery and Patents: An Update. *Recent Patents Nanomed.* 2015; 5(2): 122–145, doi: [10.2174/187791230566150616000003](https://doi.org/10.2174/187791230566150616000003).
- Sartor RB, Sartor RB. Current concepts of the etiology and pathogenesis of ulcerative colitis and Crohn’s disease. *Gastroenterol Clin North Am.* 1995; 24(3): 475–507, indexed in Pubmed: [8809232](https://pubmed.ncbi.nlm.nih.gov/8809232/).
- Ott SJ, Musfeldt M, Wenderoth DF, et al. Reduction in diversity of the colonic mucosa associated bacterial microflora in patients with active inflammatory bowel disease. *Gut.* 2004; 53(5): 685–693, doi: [10.1136/gut.2003.025403](https://doi.org/10.1136/gut.2003.025403), indexed in Pubmed: [15082587](https://pubmed.ncbi.nlm.nih.gov/15082587/).
- Frank DN, St Amand AL, Feldman RA, et al. Molecular-phylogenetic characterization of microbial community imbalances in human inflammatory bowel diseases. *Proc Natl Acad Sci U S A.* 2007; 104(34): 13780–13785, doi: [10.1073/pnas.0706625104](https://doi.org/10.1073/pnas.0706625104), indexed in Pubmed: [17699621](https://pubmed.ncbi.nlm.nih.gov/17699621/).
- Sokol H, Pigneur B, Watterlot L, et al. Faecalibacterium prausnitzii is an anti-inflammatory commensal bacterium identified by gut microbiota analysis of Crohn disease patients. *Proc Natl Acad Sci U S A.* 2008; 105(43): 16731–16736, doi: [10.1073/pnas.0804812105](https://doi.org/10.1073/pnas.0804812105), indexed in Pubmed: [18936492](https://pubmed.ncbi.nlm.nih.gov/18936492/).
- Perencevich M, Burakoff R. Use of antibiotics in the treatment of inflammatory bowel disease. *Inflamm Bowel Dis.* 2006; 12(7): 651–664, doi: [10.1097/01.MIB.0000225330.38119.c7](https://doi.org/10.1097/01.MIB.0000225330.38119.c7), indexed in Pubmed: [16804403](https://pubmed.ncbi.nlm.nih.gov/16804403/).

11. Maccaferri S, Vitali B, Klinder A, et al. Rifaximin modulates the colonic microbiota of patients with Crohn's disease: an in vitro approach using a continuous culture colonic model system. *J Antimicrob Chemother.* 2010; 65(12): 2556–2565, doi: [10.1093/jac/dkq345](https://doi.org/10.1093/jac/dkq345), indexed in Pubmed: [20852272](https://pubmed.ncbi.nlm.nih.gov/20852272/).
12. Brown CL, Smith K, Wall DM, et al. Activity of Species-specific Antibiotics Against Crohn's Disease-Associated Adherent-invasive Escherichia coli. *Inflamm Bowel Dis.* 2015; 21(10): 2372–2382, doi: [10.1097/MIB.0000000000000488](https://doi.org/10.1097/MIB.0000000000000488), indexed in Pubmed: [26177305](https://pubmed.ncbi.nlm.nih.gov/26177305/).
13. Sartor RB. Review article: the potential mechanisms of action of rifaximin in the management of inflammatory bowel diseases. *Aliment Pharmacol Ther.* 2016; 43 Suppl 1: 27–36, doi: [10.1111/apt.13436](https://doi.org/10.1111/apt.13436), indexed in Pubmed: [26618923](https://pubmed.ncbi.nlm.nih.gov/26618923/).
14. Wan YC, Li T, Han YD, et al. Effect of pregnane xenobiotic receptor activation on inflammatory bowel disease treated with rifaximin. *J Biol Regul Homeost Agents.* 2015; 29(2): 401–410, indexed in Pubmed: [26122229](https://pubmed.ncbi.nlm.nih.gov/26122229/).
15. Kolios G, Manousou P, Bourikas L, et al. Ciprofloxacin inhibits cytokine-induced nitric oxide production in human colonic epithelium. *Eur J Clin Invest.* 2006; 36(10): 720–729, doi: [10.1111/j.1365-2362.2006.01710.x](https://doi.org/10.1111/j.1365-2362.2006.01710.x), indexed in Pubmed: [16968468](https://pubmed.ncbi.nlm.nih.gov/16968468/).
16. Labro MT. Antibiotics as anti-inflammatory agents. *Curr Opin Investig Drugs.* 2002; 3(1): 61–68, indexed in Pubmed: [12054075](https://pubmed.ncbi.nlm.nih.gov/12054075/).
17. Huckle AW, Fairclough LC, Todd I. Prophylactic Antibiotic Use in COPD and the Potential Anti-Inflammatory Activities of Antibiotics. *Respir Care.* 2018; 63(5): 609–619, doi: [10.4187/respcare.05943](https://doi.org/10.4187/respcare.05943), indexed in Pubmed: [29463692](https://pubmed.ncbi.nlm.nih.gov/29463692/).
18. Rosette C, Buendia-Laysa F, Patkar S, et al. Anti-inflammatory and immunomodulatory activities of rifamycin SV. *Int J Antimicrob Agents.* 2013; 42(2): 182–186, doi: [10.1016/j.ijantimicag.2013.04.020](https://doi.org/10.1016/j.ijantimicag.2013.04.020), indexed in Pubmed: [23756321](https://pubmed.ncbi.nlm.nih.gov/23756321/).
19. Mostafa T, Badra G, Abdallah M. The efficacy and the immunomodulatory effect of rifaximin in prophylaxis of spontaneous bacterial peritonitis in cirrhotic Egyptian patients. *Turk J Gastroenterol.* 2015; 26(2): 163–169, doi: [10.5152/tjg.2015.7782](https://doi.org/10.5152/tjg.2015.7782), indexed in Pubmed: [25835116](https://pubmed.ncbi.nlm.nih.gov/25835116/).
20. Scarpignato C, Pelosini I. Rifaximin, a poorly absorbed antibiotic: pharmacology and clinical potential. *Chemotherapy.* 2005; 51 Suppl 1: 36–66, doi: [10.1159/000081990](https://doi.org/10.1159/000081990), indexed in Pubmed: [15855748](https://pubmed.ncbi.nlm.nih.gov/15855748/).
21. Ojetti V, Lauritano EC, Barbaro F, et al. Rifaximin pharmacology and clinical implications. *Expert Opin Drug Metab Toxicol.* 2009; 5(6): 675–682, doi: [10.1517/17425250902973695](https://doi.org/10.1517/17425250902973695), indexed in Pubmed: [19442033](https://pubmed.ncbi.nlm.nih.gov/19442033/).
22. Venturini AP. Pharmacokinetics of L/105, a new rifamycin, in rats and dogs, after oral administration. *Chemotherapy.* 1983; 29(1): 1–3, doi: [10.1159/000238165](https://doi.org/10.1159/000238165), indexed in Pubmed: [6549601](https://pubmed.ncbi.nlm.nih.gov/6549601/).
23. Yang J, Lee HR, Low K, et al. Rifaximin versus other antibiotics in the primary treatment and retreatment of bacterial overgrowth in IBS. *Dig Dis Sci.* 2008; 53(1): 169–174, doi: [10.1007/s10620-007-9839-8](https://doi.org/10.1007/s10620-007-9839-8), indexed in Pubmed: [17520365](https://pubmed.ncbi.nlm.nih.gov/17520365/).
24. Guslandi M, Guslandi M, Guslandi M, et al. Antibiotics for inflammatory bowel disease: do they work? *Eur J Gastroenterol Hepatol.* 2005; 17(2): 145–147, doi: [10.1097/00042737-200502000-00003](https://doi.org/10.1097/00042737-200502000-00003), indexed in Pubmed: [15674090](https://pubmed.ncbi.nlm.nih.gov/15674090/).
25. Prantera C, Lochs H, Grimaldi M, et al. Retic Study Group (Rifaximin-Eir Treatment in Crohn's Disease). Rifaximin-extended intestinal release induces remission in patients with moderately active Crohn's disease. *Gastroenterology.* 2012; 142(3): 473–481.e4, doi: [10.1053/j.gastro.2011.11.032](https://doi.org/10.1053/j.gastro.2011.11.032), indexed in Pubmed: [22155172](https://pubmed.ncbi.nlm.nih.gov/22155172/).
26. Shayto RH, Abou Mrad R, Sharara AI. Use of rifaximin in gastrointestinal and liver diseases. *World J Gastroenterol.* 2016; 22(29): 6638–6651, doi: [10.3748/wjg.v22.i29.6638](https://doi.org/10.3748/wjg.v22.i29.6638), indexed in Pubmed: [27547007](https://pubmed.ncbi.nlm.nih.gov/27547007/).
27. Ledder O. Antibiotics in inflammatory bowel diseases: do we know what we're doing? *Transl Pediatr.* 2019; 8(1): 42–55, doi: [10.21037/tp.2018.11.02](https://doi.org/10.21037/tp.2018.11.02), indexed in Pubmed: [30881898](https://pubmed.ncbi.nlm.nih.gov/30881898/).
28. Flint HJ, Scott KP, Duncan SH, et al. Microbial degradation of complex carbohydrates in the gut. *Gut Microbes.* 2012; 3(4): 289–306, doi: [10.4161/gmic.19897](https://doi.org/10.4161/gmic.19897), indexed in Pubmed: [22572875](https://pubmed.ncbi.nlm.nih.gov/22572875/).
29. Lovegrove A, Edwards CH, De Noni I, et al. Role of polysaccharides in food, digestion, and health. *Crit Rev Food Sci Nutr.* 2017; 57(2): 237–253, doi: [10.1080/10408398.2014.939263](https://doi.org/10.1080/10408398.2014.939263), indexed in Pubmed: [25921546](https://pubmed.ncbi.nlm.nih.gov/25921546/).
30. Newton AMJ, Indana VL, Kumar J. Chronotherapeutic drug delivery of Tamarind gum, Chitosan and Okra gum controlled release colon targeted directly compressed Propranolol HCl matrix tablets and in-vitro evaluation. *Int J Biol Macromol.* 2015; 79: 290–299, doi: [10.1016/j.ijbiomac.2015.03.031](https://doi.org/10.1016/j.ijbiomac.2015.03.031), indexed in Pubmed: [25936283](https://pubmed.ncbi.nlm.nih.gov/25936283/).
31. Durai R, Rajalakshmi G, Joseph J, et al. Tamarind seed polysaccharide: A promising natural excipient for pharmaceuticals. *Int J Green Pharm.* 2012; 6(4): 270, doi: [10.4103/0973-8258.108205](https://doi.org/10.4103/0973-8258.108205).
32. Newton MJ, Prabhakaran L, Kabilan P. Drug Deliveries to Colonic Region. *Indian Pharm.* 2011; 9: PP–23.
33. Joseph J, Kanchalochana S, Rajalakshmi G, et al. Tamarind seed polysaccharide: A promising natural excipient for pharmaceuticals. *Int J Green Pharm.* 2012; 6(4): 270, doi: [10.4103/0973-8258.108205](https://doi.org/10.4103/0973-8258.108205).
34. Nayak A, Pal D. Functionalization of Tamarind Gum for Drug Delivery. *Funct Biopolymers.* 2017; 25–56, doi: [10.1007/978-3-319-66417-0_2](https://doi.org/10.1007/978-3-319-66417-0_2).
35. Gorbach SL. Microbiology of the Gastrointestinal Tract. In: Baron S, ed. *Medical Microbiology.* University of Texas Medical Branch at Galveston, Galveston 1996.
36. Jess T, Simonsen J, Nielsen NM, et al. Enteric Salmonella or Campylobacter infections and the risk of inflammatory bowel disease. *Gut.* 2011; 60(3): 318, indexed in Pubmed: [21193449](https://pubmed.ncbi.nlm.nih.gov/21193449/).
37. Mehmood R, Amaldoss MJN. Fabrication and characterisation of lavender oil — plant phospholipid based Sumatriptan succinate hybrid solid lipid nanoparticles. *Pharm Biomed Res.* 2020; 6(1): 91–104.
38. Morris G, Beck P, Herridge M, et al. Hapten-Induced Model of Chronic Inflammation and Ulceration in the Rat Colon. *Gastroenterology.* 1989; 96(2): 795–803, doi: [10.1016/s0016-5085\(89\)80079-4](https://doi.org/10.1016/s0016-5085(89)80079-4).
39. Cheng J, Shah YM, Ma X, et al. Therapeutic role of rifaximin in inflammatory bowel disease: clinical implication of human pregnane X receptor activation. *J Pharmacol Exp Ther.* 2010; 335(1): 32–41, doi: [10.1124/jpet.110.170225](https://doi.org/10.1124/jpet.110.170225), indexed in Pubmed: [20627999](https://pubmed.ncbi.nlm.nih.gov/20627999/).

40. Ohwada K. [Improvement of cardiac puncture in mice]. *Jikken Dobutsu*. 1986; 35(3): 353–355, doi: [10.1538/expanim1978.35.3_353](https://doi.org/10.1538/expanim1978.35.3_353), indexed in Pubmed: [3770089](https://pubmed.ncbi.nlm.nih.gov/3770089/).
41. Bell CJ, Gall DG, Wallace JL. Disruption of colonic electrolyte transport in experimental colitis. *Am J Physiol*. 1995; 268(4 Pt 1): G622–G630, doi: [10.1152/ajpgi.1995.268.4.G622](https://doi.org/10.1152/ajpgi.1995.268.4.G622), indexed in Pubmed: [7733288](https://pubmed.ncbi.nlm.nih.gov/7733288/).
42. Beutler E, Duron O, Kelly BM. Improved method for the determination of blood glutathione. *J Lab Clin Med*. 1963; 61: 882–888, indexed in Pubmed: [13967893](https://pubmed.ncbi.nlm.nih.gov/13967893/).
43. Buege J, Aust S. [30] Microsomal lipid peroxidation. *Meth Enzymol*. 1978: 302–310, doi: [10.1016/s0076-6879\(78\)52032-6](https://doi.org/10.1016/s0076-6879(78)52032-6).
44. Miranda K, Espey M, Wink D. A Rapid, Simple Spectrophotometric Method for Simultaneous Detection of Nitrate and Nitrite. *Nitric Oxide*. 2001; 5(1): 62–71, doi: [10.1006/niox.2000.0319](https://doi.org/10.1006/niox.2000.0319).
45. Krawisz JE, Sharon P, Stenson WF. Quantitative assay for acute intestinal inflammation based on myeloperoxidase activity. *Gastroenterology*. 1984; 87(6): 1344–1350, doi: [10.1016/0016-5085\(84\)90202-6](https://doi.org/10.1016/0016-5085(84)90202-6).
46. Fontana M, Mosca L, Rosei MA. Interaction of enkephalins with oxyradicals. *Biochem Pharmacol*. 2001; 61(10): 1253–1257, doi: [10.1016/s0006-2952\(01\)00565-2](https://doi.org/10.1016/s0006-2952(01)00565-2), indexed in Pubmed: [11322929](https://pubmed.ncbi.nlm.nih.gov/11322929/).
47. Arab HH, Al-Shorbagy MY, Abdallah DM, et al. Telmisartan attenuates colon inflammation, oxidative perturbations and apoptosis in a rat model of experimental inflammatory bowel disease. *PLoS One*. 2014; 9(5): e97193, doi: [10.1371/journal.pone.0097193](https://doi.org/10.1371/journal.pone.0097193), indexed in Pubmed: [24831514](https://pubmed.ncbi.nlm.nih.gov/24831514/).
48. Harries AD, Fitzsimons E, Fifield R, et al. Platelet count: a simple measure of activity in Crohn's disease. *Br Med J (Clin Res Ed)*. 1983; 286(6376): 1476, doi: [10.1136/bmj.286.6376.1476](https://doi.org/10.1136/bmj.286.6376.1476), indexed in Pubmed: [6405846](https://pubmed.ncbi.nlm.nih.gov/6405846/).
49. Li L, Xu P, Zhang Z, et al. Platelets can reflect the severity of Crohn's disease without the effect of anemia. *Clinics (Sao Paulo)*. 2020; 75: e1596, doi: [10.6061/clinics/2020/e1596](https://doi.org/10.6061/clinics/2020/e1596), indexed in Pubmed: [32667493](https://pubmed.ncbi.nlm.nih.gov/32667493/).
50. Collins CE, Rampton DS. Review article: platelets in inflammatory bowel disease — pathogenetic role and therapeutic implications. *Aliment Pharmacol Ther*. 1997; 11(2): 237–247, doi: [10.1046/j.1365-2036.1997.153328000.x](https://doi.org/10.1046/j.1365-2036.1997.153328000.x), indexed in Pubmed: [9146760](https://pubmed.ncbi.nlm.nih.gov/9146760/).
51. Yan SLS, Russell J, Harris NR, et al. Platelet abnormalities during colonic inflammation. *Inflamm Bowel Dis*. 2013; 19(6): 1245–1253, doi: [10.1097/MIB.0b013e318281f3df](https://doi.org/10.1097/MIB.0b013e318281f3df), indexed in Pubmed: [23518812](https://pubmed.ncbi.nlm.nih.gov/23518812/).
52. Brazil JC, Louis NA, Parkos CA. The role of polymorphonuclear leukocyte trafficking in the perpetuation of inflammation during inflammatory bowel disease. *Inflamm Bowel Dis*. 2013; 19(7): 1556–1565, doi: [10.1097/MIB.0b013e318281f54e](https://doi.org/10.1097/MIB.0b013e318281f54e), indexed in Pubmed: [23598816](https://pubmed.ncbi.nlm.nih.gov/23598816/).
53. Balmus IM, Ciobica A, Trifan A, et al. The implications of oxidative stress and antioxidant therapies in Inflammatory Bowel Disease: Clinical aspects and animal models. *Saudi J Gastroenterol*. 2016; 22(1): 3–17, doi: [10.4103/1319-3767.173753](https://doi.org/10.4103/1319-3767.173753), indexed in Pubmed: [26831601](https://pubmed.ncbi.nlm.nih.gov/26831601/).
54. Guan G, Lan S. Implications of Antioxidant Systems in Inflammatory Bowel Disease. *Biomed Res Int*. 2018; 2018: 1290179, doi: [10.1155/2018/1290179](https://doi.org/10.1155/2018/1290179), indexed in Pubmed: [29854724](https://pubmed.ncbi.nlm.nih.gov/29854724/).
55. Ighodaro OM, Akinloye OA. First line defence antioxidants-superoxide dismutase (SOD), catalase (CAT) and glutathione peroxidase (GPX): Their fundamental role in the entire antioxidant defence grid. *Alexandria J M*. 2019; 54(4): 287–293, doi: [10.1016/j.ajme.2017.09.001](https://doi.org/10.1016/j.ajme.2017.09.001).
56. Docamo R, Moreno SNJ. 17 — Biochemistry of *Trypanosoma cruzi*. In: Telleria J, Tibayrenc M. ed. *American Trypanosomiasis Chagas Disease*. 2nd ed. Elsevier, London 2017: 371–400.
57. Biasi F, Leonarduzzi G, Oteiza PI, et al. Inflammatory bowel disease: mechanisms, redox considerations, and therapeutic targets. *Antioxid Redox Signal*. 2013; 19(14): 1711–1747, doi: [10.1089/ars.2012.4530](https://doi.org/10.1089/ars.2012.4530), indexed in Pubmed: [23305298](https://pubmed.ncbi.nlm.nih.gov/23305298/).
58. Hao G, Xu Z, Li Li. Manipulating extracellular tumour pH: an effective target for cancer therapy. *RSC Adv*. 2018; 8(39): 22182–22192, doi: [10.1039/c8ra02095g](https://doi.org/10.1039/c8ra02095g).
59. Mårtensson J, Jain A, Meister A. Glutathione is required for intestinal function. *Proc Natl Acad Sci USA*. 1990; 87(5): 1715–1719, doi: [10.1073/pnas.87.5.1715](https://doi.org/10.1073/pnas.87.5.1715), indexed in Pubmed: [2308931](https://pubmed.ncbi.nlm.nih.gov/2308931/).
60. Babbs CF. Oxygen radicals in ulcerative colitis. *Free Radic Biol Med*. 1992; 13(2): 169–181, doi: [10.1016/0891-5849\(92\)90079-v](https://doi.org/10.1016/0891-5849(92)90079-v), indexed in Pubmed: [1355459](https://pubmed.ncbi.nlm.nih.gov/1355459/).
61. Joo M, Kim HS, Kwon TH, et al. Anti-inflammatory Effects of Flavonoids on TNBS-induced Colitis of Rats. *Korean J Physiol Pharmacol*. 2015; 19(1): 43–50, doi: [10.4196/kjpp.2015.19.1.43](https://doi.org/10.4196/kjpp.2015.19.1.43), indexed in Pubmed: [25605996](https://pubmed.ncbi.nlm.nih.gov/25605996/).
62. Hansberry DR, Shah K, Agarwal P, et al. Fecal Myeloperoxidase as a Biomarker for Inflammatory Bowel Disease. *Cureus*. 2017; 9(1): e1004, doi: [10.7759/cureus.1004](https://doi.org/10.7759/cureus.1004), indexed in Pubmed: [28286723](https://pubmed.ncbi.nlm.nih.gov/28286723/).
63. Lau D, Baldus S. Myeloperoxidase and its contributory role in inflammatory vascular disease. *Pharmacol Ther*. 2006; 111(1): 16–26, doi: [10.1016/j.pharmthera.2005.06.023](https://doi.org/10.1016/j.pharmthera.2005.06.023), indexed in Pubmed: [16476484](https://pubmed.ncbi.nlm.nih.gov/16476484/).
64. Pattison DJ, Davies MJ. Reactions of myeloperoxidase-derived oxidants with biological substrates: gaining chemical insight into human inflammatory diseases. *Curr Med Chem*. 2006; 13(27): 3271–3290, doi: [10.2174/092986706778773095](https://doi.org/10.2174/092986706778773095), indexed in Pubmed: [17168851](https://pubmed.ncbi.nlm.nih.gov/17168851/).
65. Barone FC, Hillegass LM, Tzimas MN, et al. Time-related changes in myeloperoxidase activity and leukotriene B4 receptor binding reflect leukocyte influx in cerebral focal stroke. *Mol Chem Neuropathol*. 1995; 24(1): 13–30, doi: [10.1007/BF03160109](https://doi.org/10.1007/BF03160109), indexed in Pubmed: [7755844](https://pubmed.ncbi.nlm.nih.gov/7755844/).
66. Antoniou E, Margonis GA, Angelou A, et al. The TNBS-induced colitis animal model: An overview. *Ann Med Surg (Lond)*. 2016; 11: 9–15, doi: [10.1016/j.amsu.2016.07.019](https://doi.org/10.1016/j.amsu.2016.07.019), indexed in Pubmed: [27656280](https://pubmed.ncbi.nlm.nih.gov/27656280/).
67. Lau D, Mollnau H, Eiserich JP, et al. Myeloperoxidase mediates neutrophil activation by association with CD11b/CD18 integrins. *Proc Natl Acad Sci U S A*. 2005; 102(2): 431–436, doi: [10.1073/pnas.0405193102](https://doi.org/10.1073/pnas.0405193102), indexed in Pubmed: [15625114](https://pubmed.ncbi.nlm.nih.gov/15625114/).
68. Khalatbary AR, Ahmadvand H. Effect of oleuropein on tissue myeloperoxidase activity in experimental spinal cord trauma. *Iran Biomed J*. 2011; 15(4): 164–167, doi: [10.6091/ibj.1026.2012](https://doi.org/10.6091/ibj.1026.2012), indexed in Pubmed: [22395142](https://pubmed.ncbi.nlm.nih.gov/22395142/).
69. Fiorucci S, Distrutti E, Mencarelli A, et al. Inhibition of intestinal bacterial translocation with rifaximin modulates lamina propria monocytic cells reactivity and protects against inflammation in a rodent model of colitis. *Digestion*. 2002; 66(4): 246–256, doi: [10.1159/000068362](https://doi.org/10.1159/000068362), indexed in Pubmed: [12592101](https://pubmed.ncbi.nlm.nih.gov/12592101/).

70. Tian T, Wang Z, Zhang J. Pathomechanisms of Oxidative Stress in Inflammatory Bowel Disease and Potential Antioxidant Therapies. *Oxid Med Cell Longev*. 2017; 2017: 4535194, doi: [10.1155/2017/4535194](https://doi.org/10.1155/2017/4535194), indexed in Pubmed: [28744337](https://pubmed.ncbi.nlm.nih.gov/28744337/).
71. Mencarelli A, Renga B, Palladino G, et al. Inhibition of NF-κB by a PXR-dependent pathway mediates counter-regulatory activities of rifaximin on innate immunity in intestinal epithelial cells. *Eur J Pharmacol*. 2011; 668(1-2): 317–324, doi: [10.1016/j.ejphar.2011.06.058](https://doi.org/10.1016/j.ejphar.2011.06.058), indexed in Pubmed: [21806984](https://pubmed.ncbi.nlm.nih.gov/21806984/).
72. Banan A, Choudhary S, Zhang Y, et al. Ethanol-induced barrier dysfunction and its prevention by growth factors in human intestinal monolayers: evidence for oxidative and cytoskeletal mechanisms. *J Pharmacol Exp Ther*. 1999; 291(3): 1075–1085, indexed in Pubmed: [10565827](https://pubmed.ncbi.nlm.nih.gov/10565827/).
73. Rao R, Baker RD, Baker SS. Inhibition of oxidant-induced barrier disruption and protein tyrosine phosphorylation in Caco-2 cell monolayers by epidermal growth factor. *Biochem Pharmacol*. 1999; 57(6): 685–695, doi: [10.1016/s0006-2952\(98\)00333-5](https://doi.org/10.1016/s0006-2952(98)00333-5), indexed in Pubmed: [10037455](https://pubmed.ncbi.nlm.nih.gov/10037455/).
74. Sartor RB. Review article: the potential mechanisms of action of rifaximin in the management of inflammatory bowel diseases. *Aliment Pharmacol Ther*. 2016; 43 Suppl 1: 27–36, doi: [10.1111/apt.13436](https://doi.org/10.1111/apt.13436), indexed in Pubmed: [26618923](https://pubmed.ncbi.nlm.nih.gov/26618923/).
75. Liu X, Wang J. Anti-inflammatory effects of iridoid glycosides fraction of *Folium syringae* leaves on TNBS-induced colitis in rats. *J Ethnopharmacol*. 2011; 133(2): 780–787, doi: [10.1016/j.jep.2010.11.010](https://doi.org/10.1016/j.jep.2010.11.010), indexed in Pubmed: [21070844](https://pubmed.ncbi.nlm.nih.gov/21070844/).
76. Song M, Xia B, Li J. Effects of topical treatment of sodium butyrate and 5-aminosalicylic acid on expression of trefoil factor 3, interleukin 1beta, and nuclear factor kappaB in trinitrobenzene sulphonic acid induced colitis in rats. *Postgrad Med J*. 2006; 82(964): 130–135, doi: [10.1136/pgmj.2005.037945](https://doi.org/10.1136/pgmj.2005.037945), indexed in Pubmed: [16461476](https://pubmed.ncbi.nlm.nih.gov/16461476/).